

Metode i metodologija u statističkoj termodinamici

Mihajlo Etinski

- Uvod
- Pregled statističke termodinamike
- Računarske simulacije
- Molekulska dinamika
- Monte Karlo metoda
- Zaključak

Uvod

Eksperiment

- Priprema uzorka
- Merenja, osmatranja
- Skupljanje podataka
- Obrada podataka

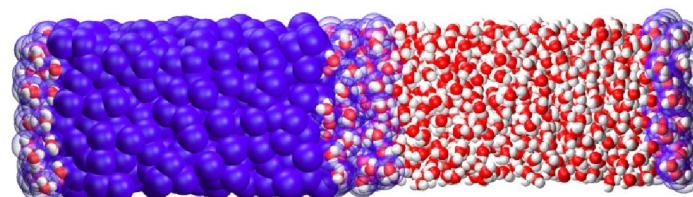
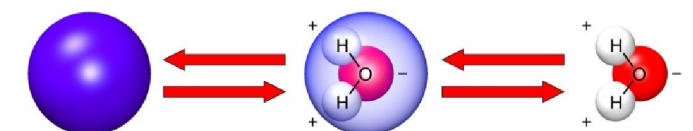
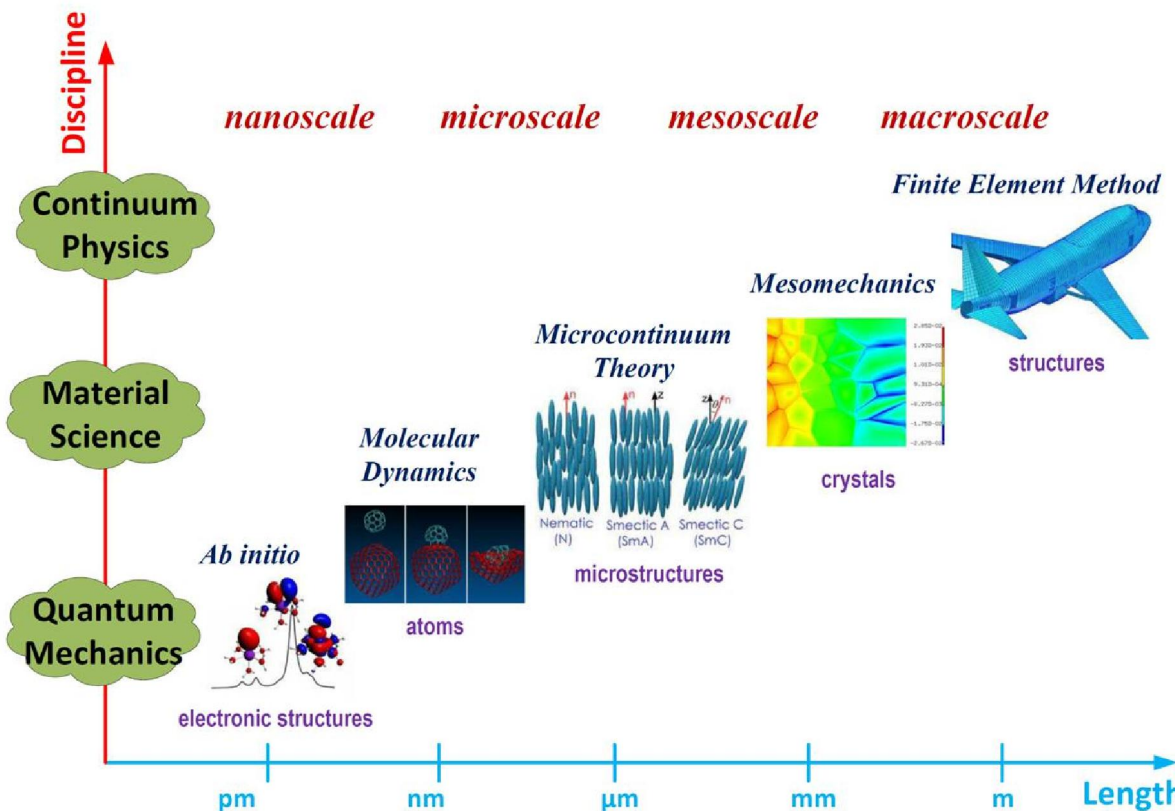
Teorija

- Razvijanje modela i hipoteza
- Predikcija eksperimenata

Računarske simulacije

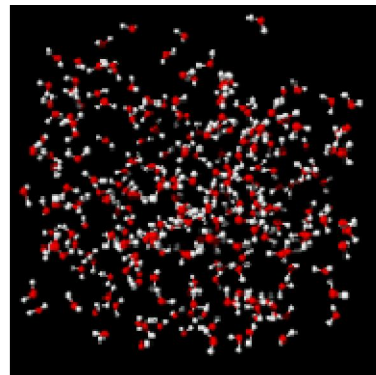
- Priprema modela
- Obrada podataka
- Testiranje teorija
- Mogućnost simulacije eksperimenata koje je teško izvesti

Sta želimo da modelujemo?

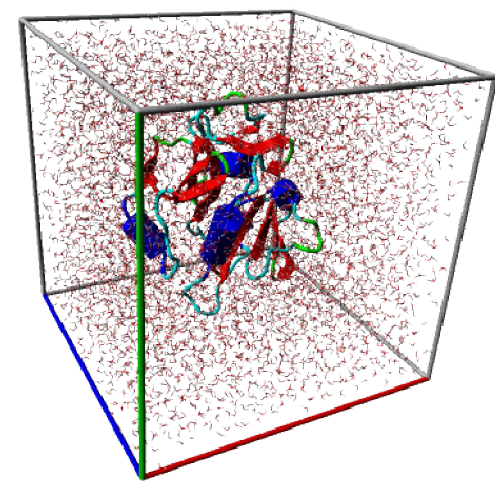


Sta želimo da modelujemo?

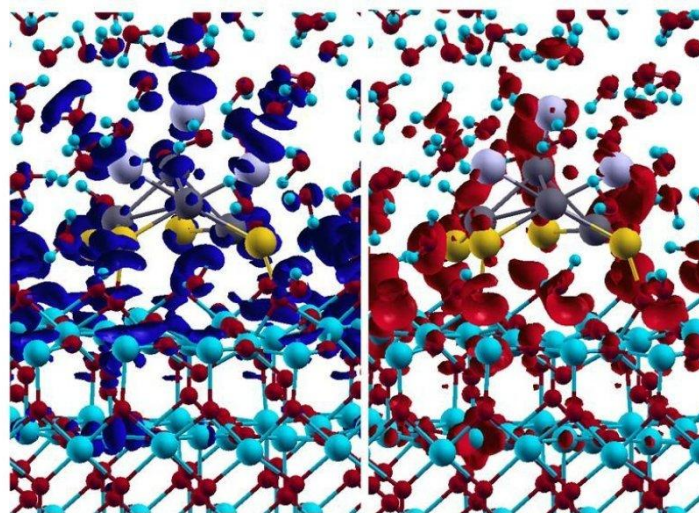
Fazni prelazi



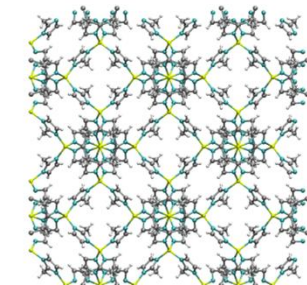
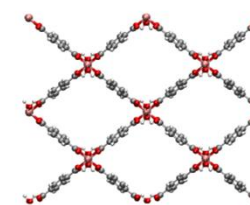
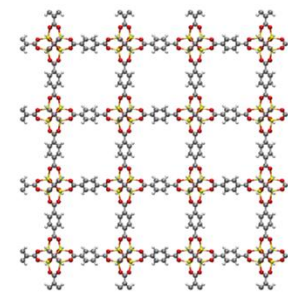
Biološke sisteme



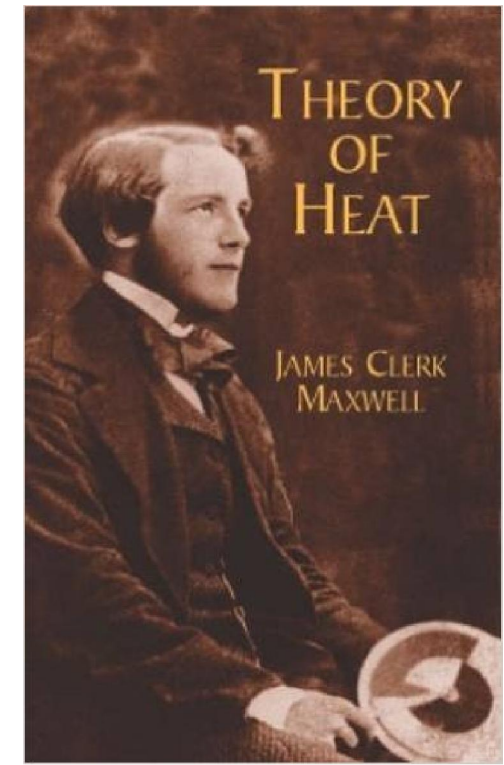
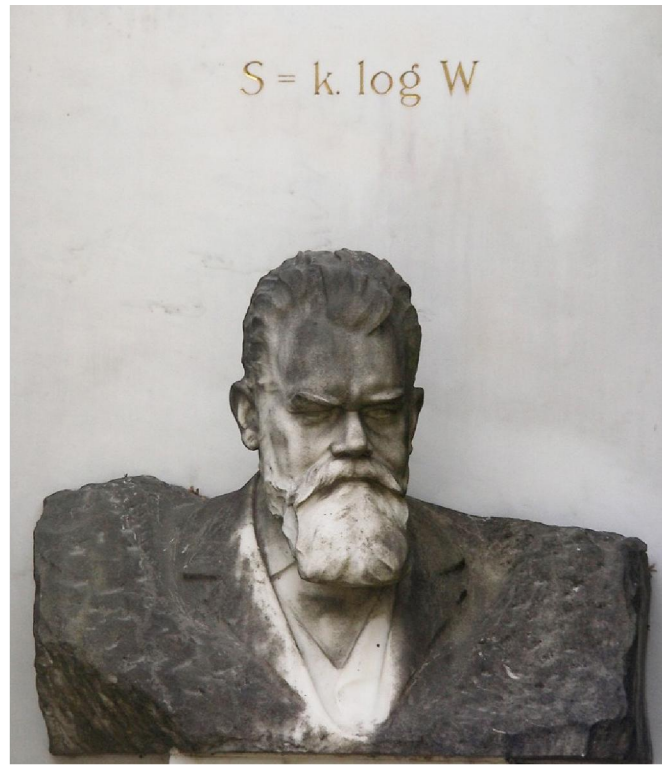
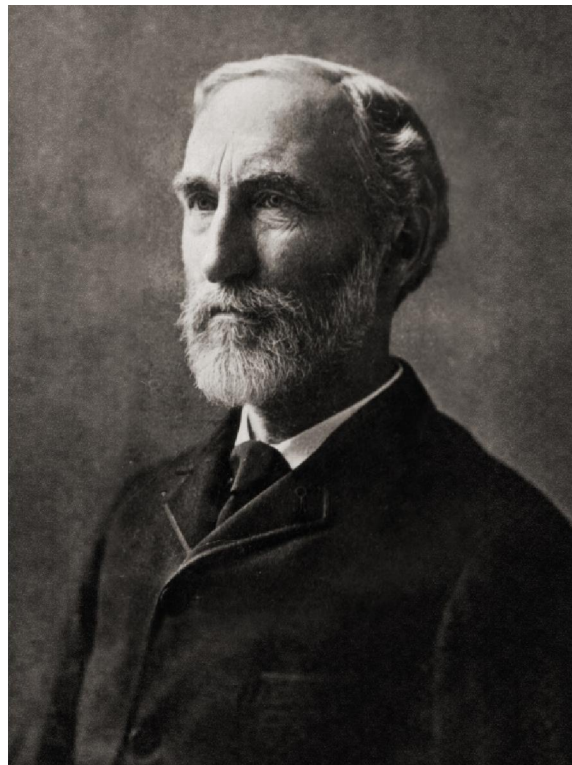
Katalitičke mehanizme



Osobine materijala



Pregled statističke termodinamike

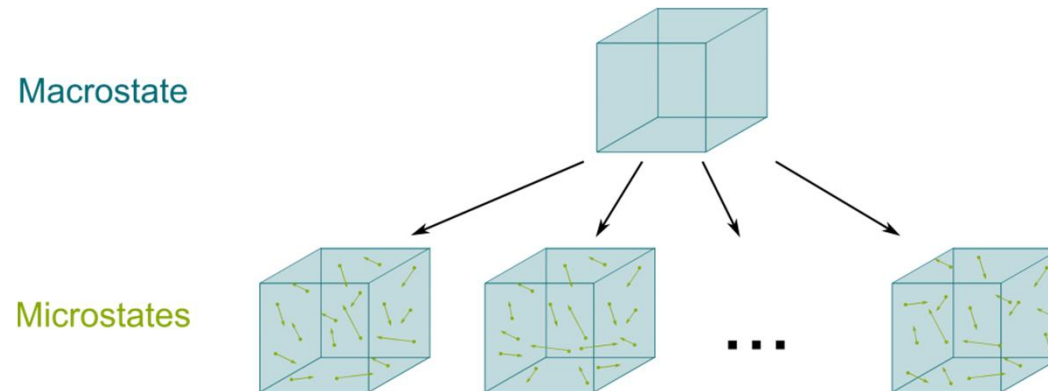


Makrokoordinate: energija, zapremina, površina, polarizacija, magnetizacija, molski brojevi komponenti, ...

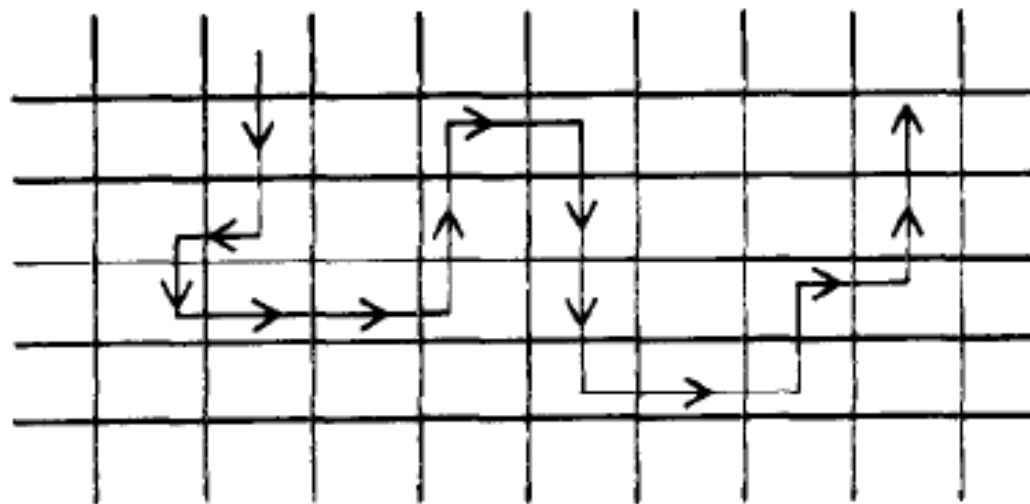
Makrostanja: (E, N, V) , (T, N, V) , (T, N, P) , (T, μ, V) , ...

Mikrokoordinate: položaji čestica

Mikrostanje: klasično i kvantno stanje



Ergodični sistemi



$$\langle A \rangle = \frac{1}{N} \sum_i^N A_i = \sum_i P_i A_i$$

Statistička termodinamika se zasniva na jednoj pretpostavci:

Sva dostupna mikrostanja izolovanog sistema su podjednako verovatna

Mikrokanonski ansabl: $S=k \ln \Gamma(E,N,V)$
 $P=1/\Gamma(E,N,V)$

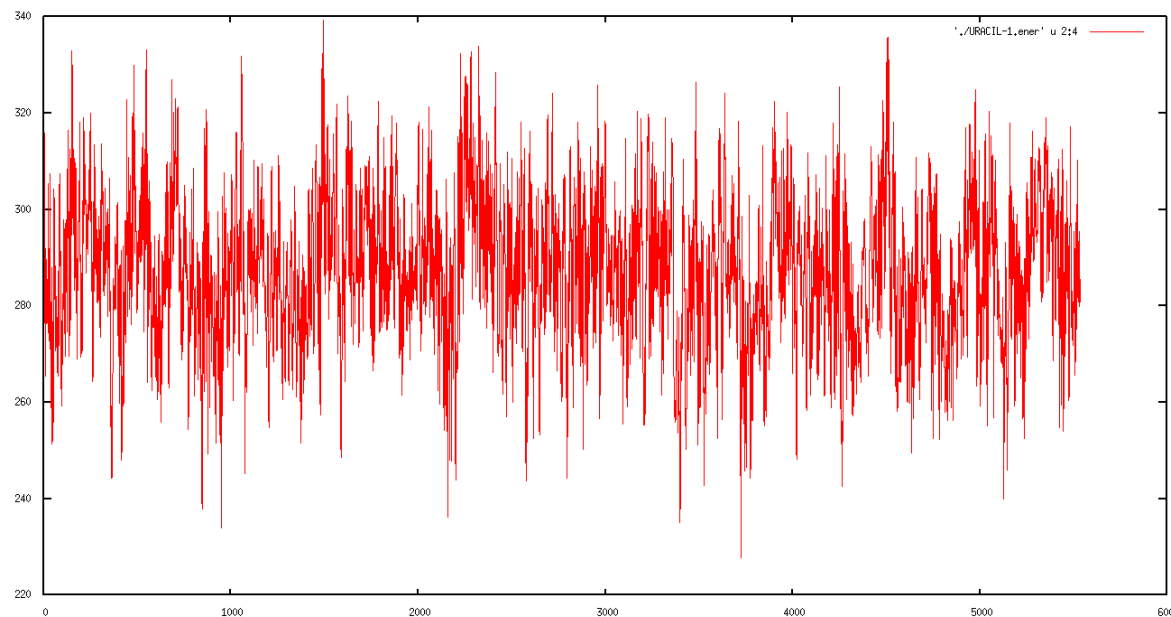
Kanonski ansabl: $F=-kT \ln Q$
 $P(E_i)=\exp(-\beta E_i)/Q$

Veliki kanonski ansabl: $\Omega=-kT \ln \Xi$
 $P(E_i,N)=\exp(-\beta E_i+\mu \beta N)/\Xi$

Particione funkcije se ne mogu izračunati osim za najjednostavnije sisteme

Računarske simulacije

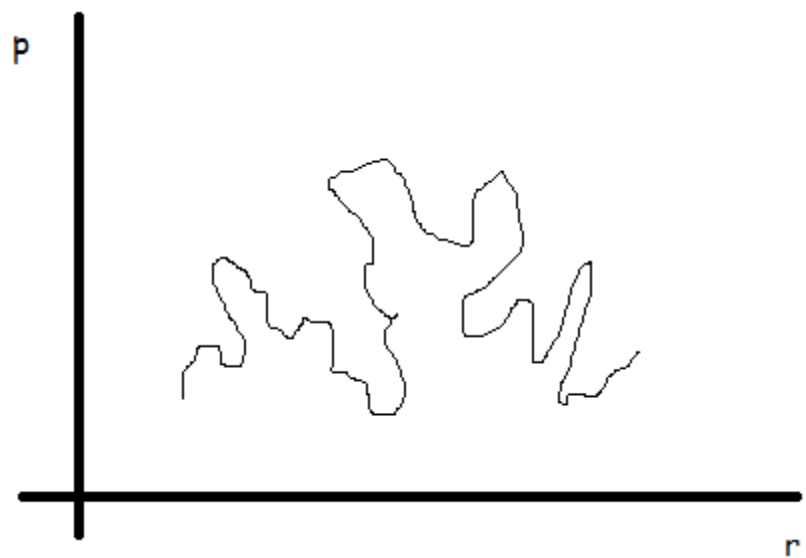
- Računarske simulacije daju egzatno rešenje u okviru korišćenog modela
- Izbor modela sistema zavisi od toga sta želimo da simuliramo
- Računarske simulacije zbog vremenskog ograničenja prouzrokovanim ograničenim računarskim resursima obično razmatraju sisteme od 100-10000 čestica i vremenske opsege od 10 ps do 100 ns
- Srednja vrednost dinamičke promenjive i njena statistička greška



Monte Karlo metod
Uzorkovanje po važnosti



Molekulska dinamika
Rešavanje Njutnovih jednačina kretanja

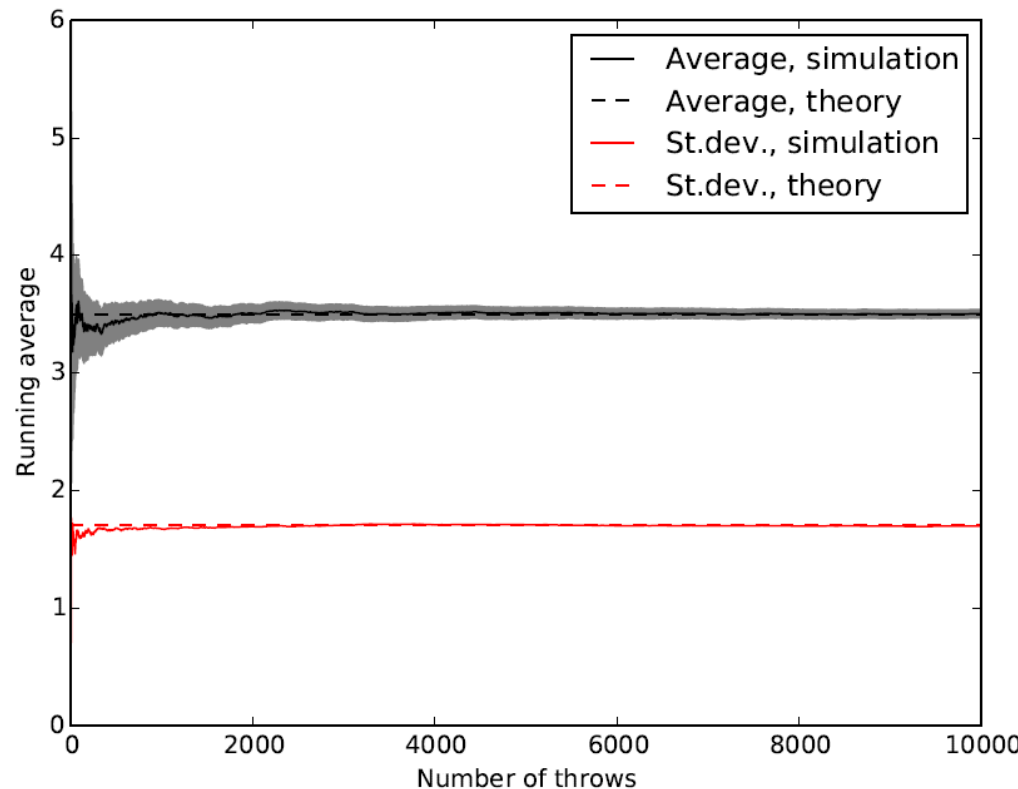


Kako proceniti kvalitet simulacije?

Primer: bacanje kockice

Srednje vrednost $\langle x \rangle = \sum i p_i x_i = 3.5$

Standardna devijacija $\sigma = \sqrt{\langle x^2 \rangle - \langle x \rangle^2} \approx 2.92$



Born-Openhajmerova aproksimacija za molekule:
Atomska jezgra se kreću na površi potencijalne energije

Kako modelovati površ potencijalne energije ?

Molekulska mehanika

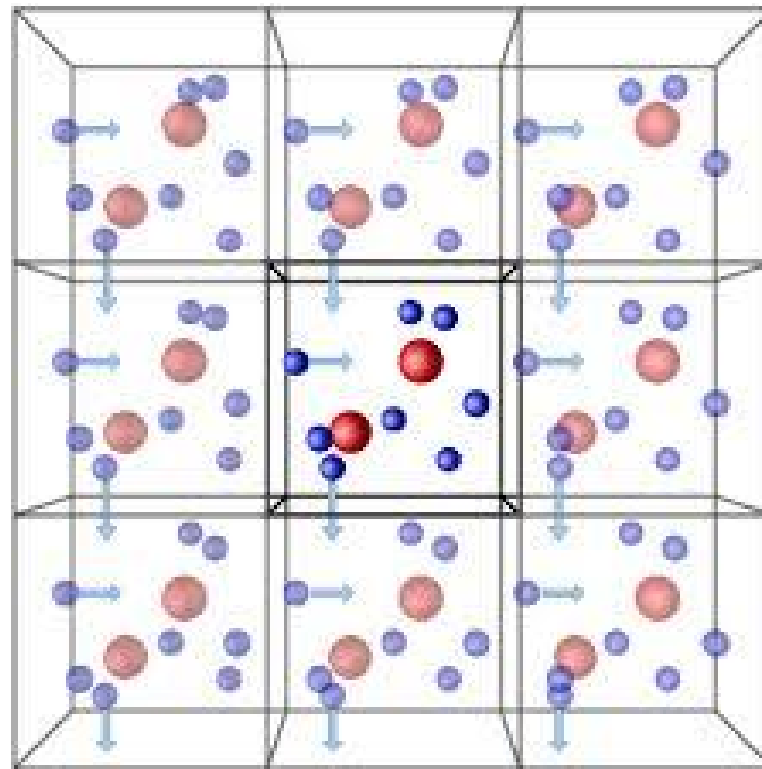
$$V = \sum_{vezes} k_r(r - r_{eq})^2 + \sum_{uglovi} k_\theta(\theta - \theta_{eq})^2 + \sum_{diedralniuglovi} \frac{1}{2}\pi_n(1 + \cos(n\varphi - \varphi_0)) + \sum_{i < j} \left(\frac{a_{ij}}{r_{ij}^{12}} - \frac{b_{ij}}{r_{ij}^6} + \frac{q_i q_j}{\epsilon r_{ij}} \right)$$

Ab initio potencijal

Potrebno je rešiti elektronsku Šredingerovu jednačinu u svakom koraku (BOMD)
Kretanje elektrona se uključuje preko fiktivnih stepeni slobode (CPMD)

Periodični uslovi

Potrebni su da bi se izbegao uticaj površinskih efekata na simulaciju



Čestice interaguju sa svim (beskonačno mnogo) replikama čestica

Ograničavanje interakcija

Da bi se izbeglo računanje interakcije sa beskonačno mnogo replika, obično se potencijali koji brzo opadaju ograničavaju do nekog rastojanja r_c . Izuzeci su Kulonov potencijal i interakcije dipolnih momenta.

Od posebnog interesa je slučaj $r_c=L/2$ - posmetra se interakcija čestice samo sa najблиžom replikom ostalih čestica

Ipak, moramo dodati korekciju za ukupnu potencijalnu energiju

$$U = \sum_{i < j} u_c(r_{ij}) + \frac{N\rho}{2} \int_{r_c}^{\infty} u(r) d^3r$$

Koraci tokom izvođenja simulacije:

Inijalizacija sistema

Uravnotežnjenje sistema

Proizvodnja rezultata

Obrada podataka

Koraci tokom izvodjenja eksperimenta:

Priprema uzorka

Merenje

Obrada podataka

Molekulska dinamika

Izračunati sile koje deluju na čestice i rešiti Njutnove jednačine kretanja

Srednja vrednost termodinamičkih promenjivih se računa koristeći vremensku usrednjenost

Mogu se računati vremenski nezavisne (termodinamičke i strukturne) ali i vremenski zavisne (kinetički koeficienti) osobine sistema

Molekulska dinamika u NVE ansamblu

Inicijalizacija:

Izabradi broj čestica, gustinu, dužinu vremenskog koraka za dinamiku,...

Izabradi početni položaj čestica. Poželjno je da se čestice ne preklapaju. Dobra početna konfiguracija je npr. kada se čestice nalaze u čvorovima jednostavne kubne kristalne rešetke

Brzine čestica u početku biramo na slučajan način, pogodno iz Maksvelove raspodele za zadatu temperaturu

Uravnoteženje:

Početno stanje je malo verovatno stanje za termodinamičke parametre koje želimo da simuliramo. Stoga je potrebno pripremiti sistem u stanje koje odgovara željenim parametrima. Tome služi uravnotežnjenje sistema.

Iako ćemo koristiti NVE ansambl za uzorkovanje stanja, pogodno je pripremiti sistem na željenu temperaturu. U tu svrhu koristimo skaliranje brzina čestica na odabranu temperaturu tokom ovog dela simulacije

Ovakvo skaliranje temperature ne oponaša NVT ansambl, ali je pogodno kao brz metod za uravnotežnjenje sistema

Integracija Njutovih jednačina:

Periodični uslovi

Ograničen i pomeren potencijal

Ograničeni LJ potencijal

$$u(r) = \begin{cases} u(r) & r \leq r_c \\ 0 & r > r_c \end{cases}$$

Ograničeni i pomereni LJ potencijal

$$u(r) = \begin{cases} u(r) - u(r_c) & r \leq r_c \\ 0 & r > r_c \end{cases}$$

Jednačine kretanja

$$\vec{r}(t + \Delta t) = \vec{r}(t) + \vec{v}(t)\Delta t + \frac{\Delta t^2}{2m} \vec{f}(t) + \frac{\Delta t^3}{3!} \ddot{\vec{r}}(t) + O(\Delta t^4)$$
$$\vec{r}(t - \Delta t) = \vec{r}(t) - \vec{v}(t)\Delta t + \frac{\Delta t^2}{2m} \vec{f}(t) - \frac{\Delta t^3}{3!} \ddot{\vec{r}}(t) + O(\Delta t^4)$$
$$\vec{r}(t + \Delta t) - \vec{r}(t - \Delta t) = 2\vec{r}(t) + \frac{\Delta t^2}{m} \vec{f}(t) + O(\Delta t^4)$$

Verleov algoritam

$$\vec{r}(t + \Delta t) \approx 2\vec{r}(t) + \vec{r}(t - \Delta t) + \frac{\Delta t^2}{m} \vec{f}(t)$$

Verleov algoritam ne koristi brzine da bi se odredili položaji čestica u sledećoj tački. Brzine se mogu odrediti na sledeći način:

$$v(t) = \frac{\vec{r}(t + \Delta t) - \vec{r}(t - \Delta t)}{2\Delta t}$$

Najviše vremena potrebno je izračunavanje sila

Molekulska dinamika u različitim ansamblima?

Ansambl	Konstantne veličine	Termodinamičke funk.
Mikrokanonski	N,V,E	$S=k \ln \Gamma(N,V,E)$
Kanonski	N,V,T	$\beta F = -\ln Q(N,V,T)$
Izobarski-izotermski	N,P,T	$\beta G = -\ln \Delta(N,P,T)$

ARTICLE

Received 23 Aug 2014 | Accepted 3 Jun 2015 | Published 13 Jul 2015

DOI: 10.1038/ncomms8696

OPEN

Evidence of liquid-liquid transition in glass-forming $\text{La}_{50}\text{Al}_{35}\text{Ni}_{15}$ melt above liquidus temperature

Wei Xu^{1,2}, Magdalena T. Sandor³, Yao Yu^{1,2}, Hai-Bo Ke⁴, Hua-Ping Zhang⁵, Mao-Zhi Li⁵, Wei-Hua Wang⁴, Lin Liu¹ & Yue Wu³

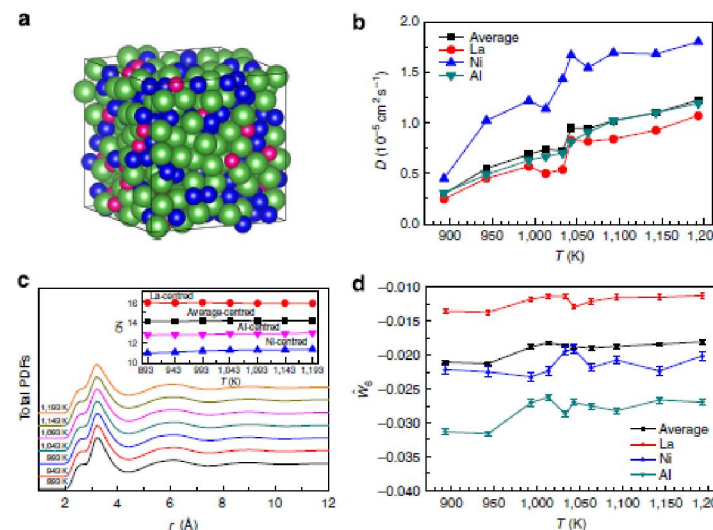


Figure 3 | Ab initio MD simulations. (a) A typical atomic configuration equilibrated in the liquid state at 1,143 K modelled by *ab initio* MD simulations. Green, blue and red balls represent La, Al and Ni, respectively. (b) Temperature-dependent diffusion coefficient of $\text{La}_{50}\text{Al}_{35}\text{Ni}_{15}$ liquid, which shows qualitative changes around 1,043 K. (c) Total pair distribution functions (PDFs) of $\text{La}_{50}\text{Al}_{35}\text{Ni}_{15}$ liquid at different temperatures. The inset shows the variation of coordination number (CN) with temperature. (d) Temperature dependence of the average \bar{W}_6 of all three elements and \bar{W}_6 of individual element. The error bars are shown along with the data symbols. The error bars were estimated from the s.d. of \bar{W}_6 in two independent MD simulations.

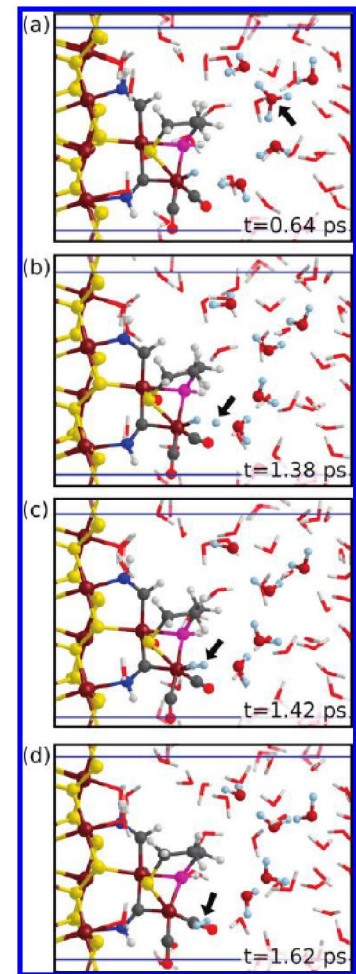
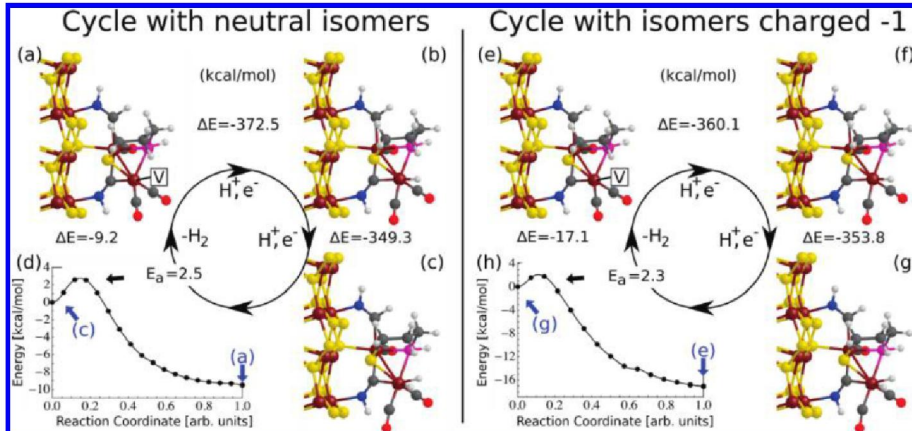
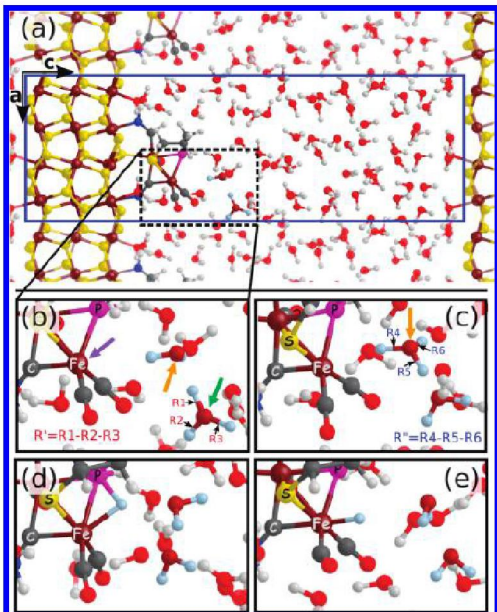
Published on Web 06/03/2010

Simulation of Electrocatalytic Hydrogen Production by a Bioinspired Catalyst Anchored to a Pyrite Electrode

Federico Zipoli,^{*,†} Roberto Car,^{†,‡} Morrel H. Cohen,^{†,§} and Annabella Selloni^{*,†}

Department of Chemistry, Princeton Institute for the Science and Technology of Materials, Princeton University, Princeton, New Jersey 08544, and Department of Physics and Astronomy, Rutgers University, Piscataway, New Jersey 08854

Received December 18, 2009; E-mail: fzipoli@princeton.edu; aselloni@princeton.edu



HIV-1 protease flaps spontaneously open and reclose in molecular dynamics simulations

Viktor Hornak*, Asim Okur†, Robert C. Rizzo*§, and Carlos Simmerling*†¶

Departments of †Chemistry and ‡Applied Mathematics and Statistics and *Center for Structural Biology, Stony Brook University, Stony Brook, NY 11794; and §Computational Science Center, Brookhaven National Laboratory, Upton, NY 11973

Edited by Janet M. Thornton, European Bioinformatics Institute, Cambridge, United Kingdom, and approved November 18, 2005 (received for review September 27, 2005)

We report unrestrained, all-atom molecular dynamics simulations of HIV-1 protease that sample large conformational changes of the active site flaps. In particular, the unliganded protease undergoes multiple conversions between the "closed" and "semiopen" forms observed in crystal structures of inhibitor-bound and unliganded protease, respectively, including reversal of flap "handedness." Simulations in the presence of a cyclic urea inhibitor yield stable closed flaps. Furthermore, we observe several events in which the flaps of the unliganded protease open to a much greater degree than observed in crystal structures and subsequently return to the semiopen state. Our data strongly support the hypothesis that the unliganded protease predominantly populates the semiopen conformation, with closed and fully open structures being a minor component of the overall ensemble. The results also provide a model for the flap opening and closing that is considered to be essential to enzyme function.

AIDS | HIV protease | molecular dynamics simulations | protein dynamics

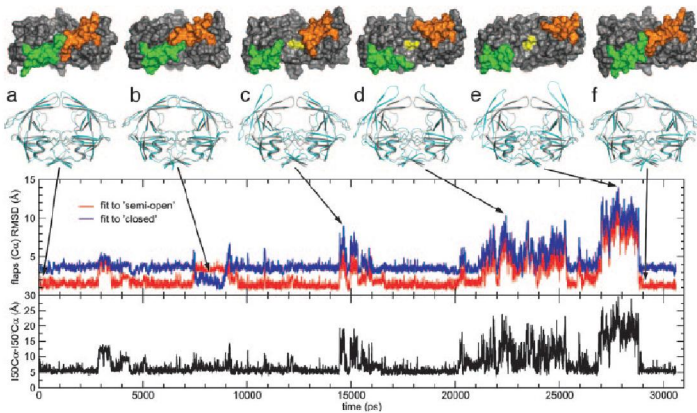


Fig. 4. Flaps RMSD and flap tips distance for free HIV-PR simulation started from a semiopen crystal structure. Snapshots (cartoon diagrams, side view) along the trajectory (cyan) are shown overlapped on the semiopen crystal structure (gray). Surface representations (top view) depict flap handedness and access to the active site, with the two flaps in green/orange and the catalytic Asp-25/25' in yellow. The semiopen conformation is equivalent (low RMSDs for red line). Note that the transiently sampled closed structure (structure b) has the flap handedness characteristic of bound (closed) crystal structures, even though flaps do not become fully pulled into the active site in this simulation. Large flap openings are sampled (structures c–e), with flap tip distances reaching ~ 30 Å and subsequently returning to the semiopen form (structures e–f).

prior computational studies have aimed at understanding flap opening dynamics. Collins *et al.* (7) reported results from activated molecular dynamics (MD) simulations in the gas phase that involved forcing the atomic coordinates for nonflap regions of a closed structure to the semiopen state. These simulations produced flap opening, but the use of restraints prevented investigation of coupling between flap and core domains (8). Scott and Schiffer (9) also observed irreversible flap opening after 3 ns of a 10-ns MD simulation in explicit water, but the extent of flap opening was not quantitatively described. Instead they focused on the flap tip regions, which "curled" back into the protein structure during the opening event, burying several hydrophobic residues. This flap curling was hypothesized to provide a key conformational trigger necessary for subsequent large-scale flap opening and therefore HIV-PR function. More recently, Hamelberg and McCammon (10) used activated dynamics to produce flap opening in HIV-PR. Perryman *et al.* (11) reported dynamics of unbound V82F/I84V mutant in which the

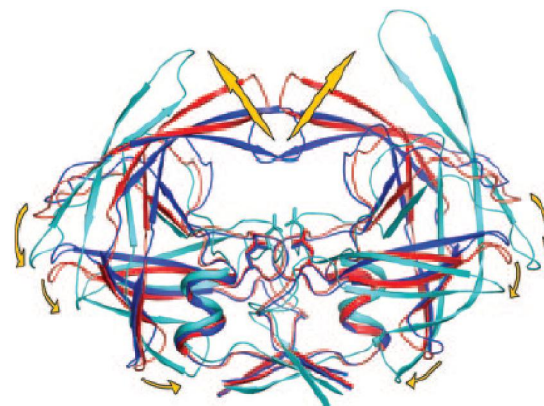
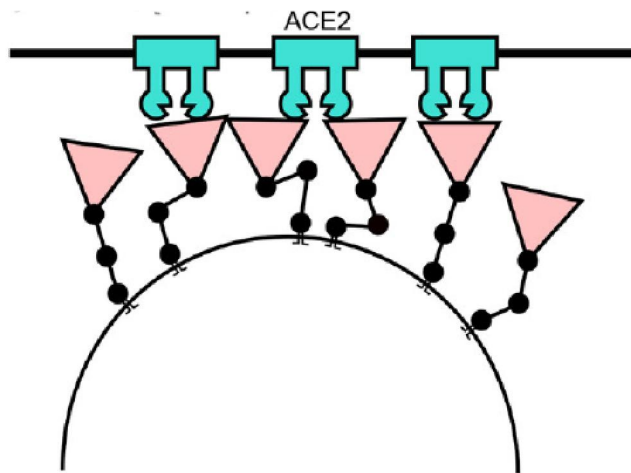
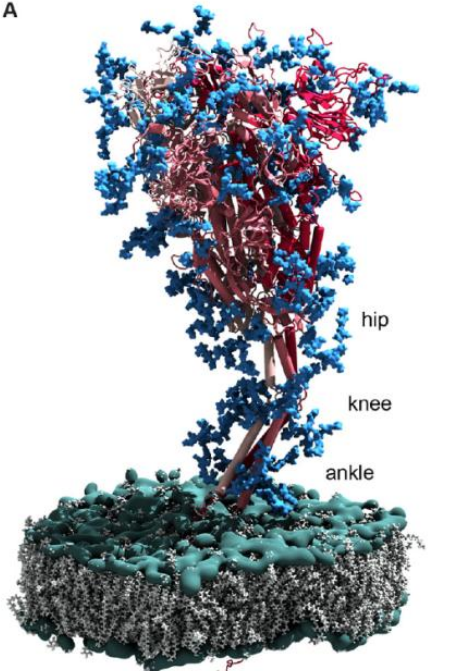


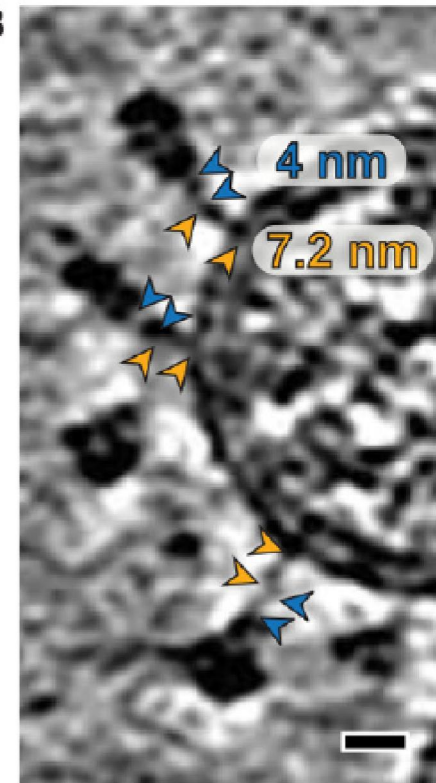
Fig. 6. Three forms of HIV-1 protease: closed (blue, PDB ID code 1HVR), semiopen (red, PDB ID code 1HHP), and open (cyan, our model). We observe opening/closing wherein the flap elbows and exposed ends of fulcrum and cantilever move down and toward the terminal β -sheet dimer interface (indicated by yellow arrows). Examination of closed and semiopen crystal structures reveals differences in those regions that are smaller in magnitude but in agreement with the direction of changes seen during opening.

~ 40 S proteina po virusu
Antitela treba da se vezu za S protein

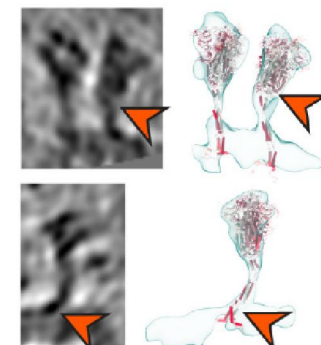
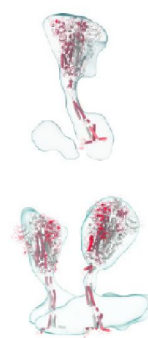
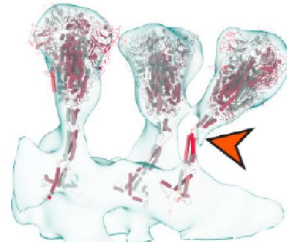
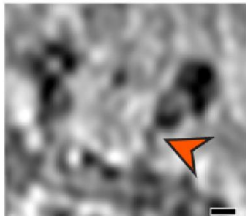
A



B



Sistem se sastoji od 4 S proteina zakacena za membranu virusa u vodenom rastvoru. 2.5 duga MD simulacija sa 4.1 miliona atoma. NPT ansambl, T=310 K, P=1 atm.



B. Turoňová et al., *Science*
10.1126/science.abd5223 (2020).

Coarse-grained molecular dynamics simulations of membrane proteins and peptides

Peter J. Bond, John Holyoake, Anthony Ivetac, Syma Khalid, Mark S.P. Sansom *

Department of Biochemistry, University of Oxford, South Parks Road Oxford, OX1 3QU, UK

Received 22 April 2006; received in revised form 30 July 2006; accepted 3 October 2006

Available online 20 October 2006

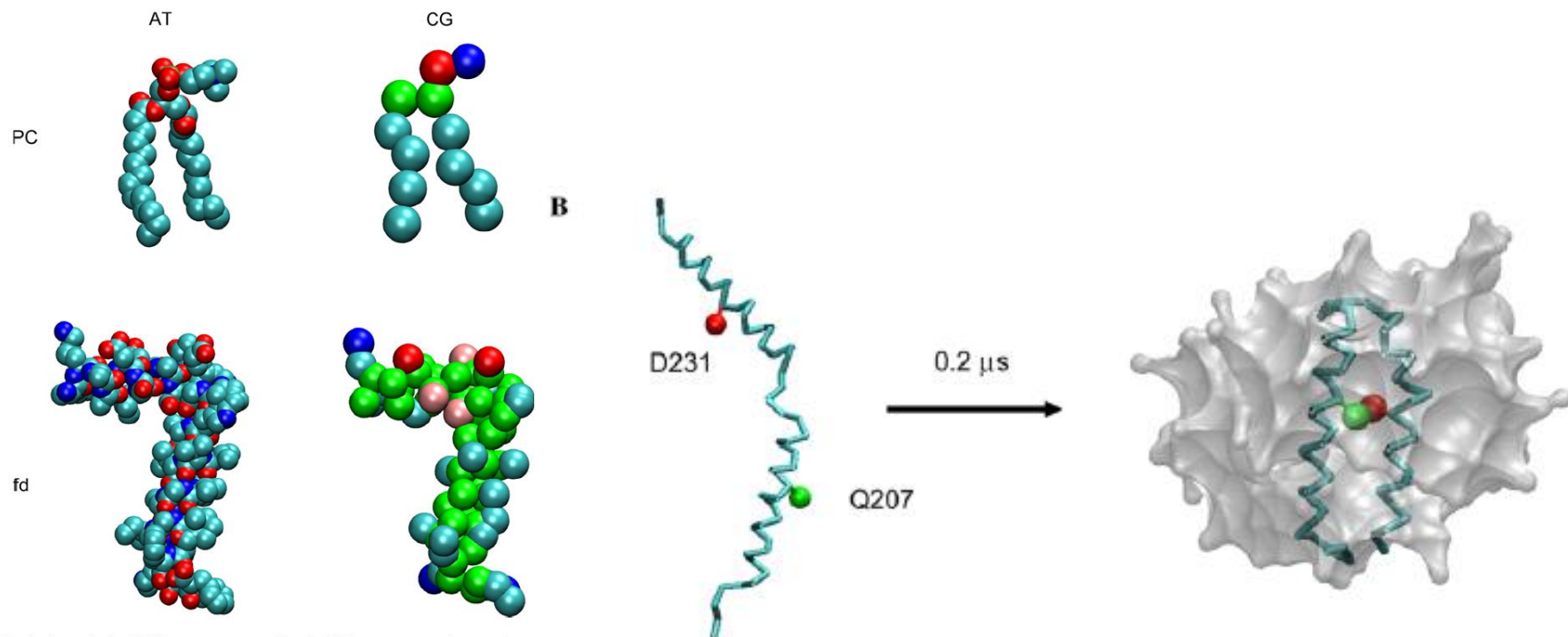


Fig. 1. Atomistic (AT) vs. coarse-grained (CG) representations of molecules. Two lipid molecule structures are shown for phosphatidyl choline (PC), namely DMPC (atomistic) and DPPC. (CG). The fd phage coat protein is also shown in AT and CG format. In all diagrams the molecules are shown in spacefilling format. In the AT models the atoms are coloured using the CPK convention. In the CG models the particles are coloured according to the following scheme: green, mixed polar/nonpolar particle; cyan, hydrophobic particle; red/blue, negative/positive, charged particle; and pink, polar particle.

Monte Karlo metod

Srednja vrednost dinamičke promenjive u kanonskom ansamblu:

$$\langle A \rangle = \frac{\int A e^{-\beta H} d^3 r_1 \dots d^3 p_1}{\int e^{-\beta H} d^3 r_1 \dots d^3 p_1}$$

Ako dinamička promenjiva zavisi samo od prostornih koordinata:

$$\langle A \rangle = \frac{\int A e^{-\beta V} d^3 r_1 \dots d^3 r_N}{\int e^{-\beta V} d^3 r_1 \dots d^3 r_N}$$

$$I = \int_a^b f(x) dx = \langle f(x) \rangle (b - a)$$

Za numeričku integraciju 1-d integrala potrebno je odabrati N ekvidistatnih tačaka u intervalu (a,b) i vrednost funkcije u tim tačkama.

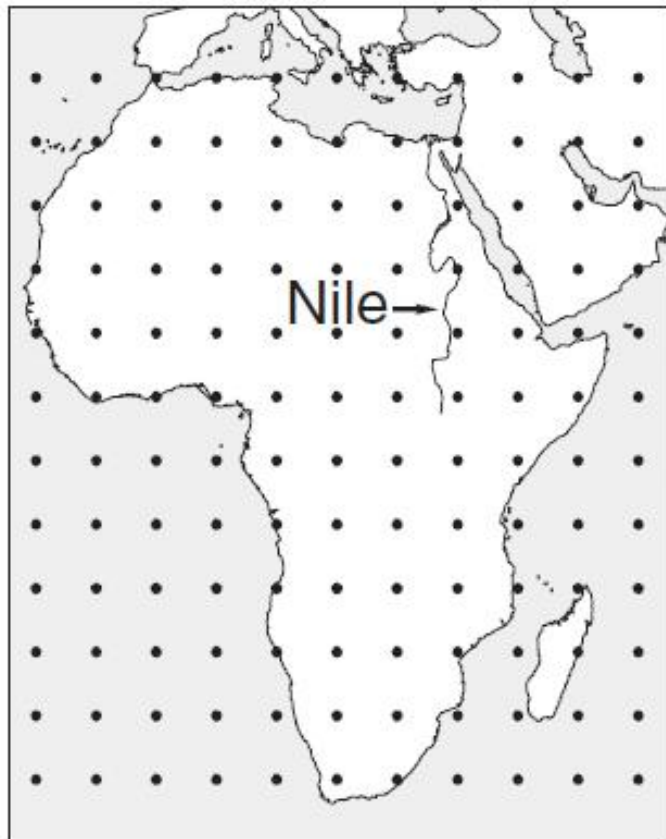
Monte Karlo integracija se zasniva na uzorkovanju N tačaka koristeći uniformnu raspodelu verovatnoće

$$\langle f(x) \rangle = \frac{1}{N} \sum_i f(x_i)$$

Za numeričku integraciju d-dimenzionalnog integrala potrebno je N^d tačaka, N je broj ekvidistantnih tačaka duž jedne dimenzije. Mnogo manje tačaka je potrebno ako koristimo Monte Karlo metod

Uzorkovanje po važnosti - često nisu sve tačke podjednako važne

Kolika je prosečna dubina Nila?



U molekulskim sistemima jako veliki broj konfiguracija ima veoma malu verovatnoću jer je njihova potencijala energija ogromna.

Potrebno je rešiti:

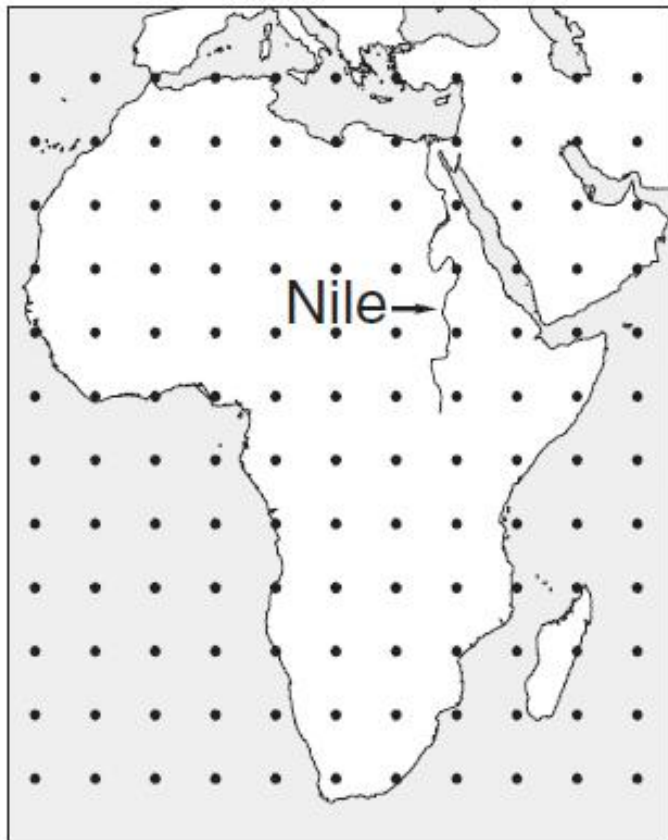
$$\langle A \rangle = \frac{\int A e^{-\beta V} d^3 r_1 \dots d^3 r_N}{\int e^{-\beta V} d^3 r_1 \dots d^3 r_N}$$

Bilo bi sjajno ako bi mogli da uzorkujemo tačke direktno iz Boltzmanove raspodele

$$\langle A \rangle = \int A P_N(\vec{r}_1 \dots \vec{r}_N) d^3 r_1 \dots d^3 r_N$$

Problem je to što ne znamo vrednost partacione funkcije. Ono sto znamo za svaku konfiguraciju je samo relativna verovatnoća u odnosu na drugu konfiguraciju

$$\frac{P_N(1)}{P_N(2)} = e^{-\beta(V(1)-V(2))}$$



Kako efikasno odrediti dubinu Nila?

Želeli bismo da uzorkujemo samo tačke gde se nalazi Nil. Počnimo od jedne tačke gde se nalazi Nil. Izaberimo sledeću tačku tako što ćemo na slučajan način izabrati tačku u blizini i utvrditi da li se nalazi na Nilu. Ako se nalazi, uvrstićemo je u srednju vrednost i pomerićemo se u tu tačku, u suprotnom uvrstimo predhodnu tačku ponovo u srednju vrednost i ostati u toj tački. Tu proceduru ponavljamo dovoljan broj puta.

Metropolisov Monte Karlo metod

Stanja iz konfiguracionog prostora uzorkujemo na sledeći način:

Na slučajan način izaberemo novu konfiguraciju koja sa nalazi u blizini predhodne konfiguracije. Ako je njena potencijalna energija manja od predhodne potencijalne energije, prihvatamo novu konfiguraciju. U slučaju da nije manja, računamo vrednost $\exp(-\beta(V(\text{novo})-V(\text{staro}))$ i opoređujemo taj broj sa slučajnim brojem izvučenim iz uniformne raspodele. U slučaju da je uniformni broj manji od ove vrednosti uzimamo novu konfiguraciju, u suprotnom zadržavamo staru konfiguraciju. Proceduru ponavljamo dovoljan broj puta. Očekivana vrednost dinamičke promenjive predstavlja srednju vrednost promenjive u svim dobijenim konfiguracijama.

Detaljan balans (mikroskopska ravnoteža)

U termodinamičkoj ravnoteži ukupan broj sistema koji se kreću iz konfiguracije a u b, $K(a \rightarrow b)$ treba da je jednak broju sistema koji se kreću iz b u a, $K(a \leftarrow b)$.

$$K(a \rightarrow b) = K(a \leftarrow b)$$

$$K(a \rightarrow b) = N(a) \times \alpha(a \rightarrow b) \times acc(a \rightarrow b)$$

$N(a)$: ukupan broj sistema ansambla u konfiguraciji a, proporcionalan $\exp(-\beta V(a))$

$\alpha(a \rightarrow b)$: a priori verovatnoća da se generiše pomeranje a \rightarrow b

$acc(a \rightarrow b)$: verovatnoća da se prihvati pomeranje a \rightarrow b

U Metropolisovoj verziji $\alpha(a \rightarrow b) = \alpha(a \leftarrow b)$

$$\frac{acc(a \rightarrow b)}{acc(a \leftarrow b)} = \frac{N(b)}{N(a)} = e^{-\beta(V(b)-V(a))}$$

Zbog uslova mikroskopske ravnoteže, Monte Karlo simulacije mogu da se koriste da bi se odredile ravnotežne osobine sistema ali ne i neravnotežne

Na koji način se bira nova konfiguracija?

Možemo pomerati sve atoma od jednom ili izabrati samo jedan atom i njega pomeriti

Rastojanje za koje se pomeraju atomi ne treba da je premalo ni preveliko. Kada je malo konfiguracioni prostor se sporo ispituje, kada je veliko, mnogo konfiguracija biva odbačeno.

Za translaciona pomeranja:

$$x_b = x_a + \Delta * (\text{rand} - 0.5)$$

$$y_b = y_a + \Delta * (\text{rand} - 0.5)$$

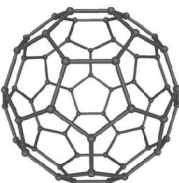
$$z_b = z_a + \Delta * (\text{rand} - 0.5)$$

Monte Karlo metod u različitim ansamblima

Ansambl	Konstantne veličine	Termodinamičke funk.
Kanonski	N,V,T	$\beta F = -\ln Q(N,V,T)$
Izobarski-izotermski	N,P,T	$\beta G = -\ln \Delta(N,P,T)$
Veliki kanonski	μ, V, T	$\beta \Omega = -\ln \Xi(\mu, V, T)$

Pod uslovom konstantnog pritiska zapremina simulacione kutije se može menjati tako što se sve koordinate čestica skaliraju konstantnim faktorom

Pod uslovom konstantnog hemijskog potencijala broj čestica se može menjati tako što se ubaci ili uzme čestica iz simulacione kutije



Does C_{60} have a liquid phase?

M. H. J. Hagen*, E. J. Meijer*, G. C. A. M. Moolj*,
D. Frenkel*† & H. N. W. Lekkerkerker‡

* FOM Institute for Atomic and Molecular Physics, Kruislaan 407,
1098 SJ Amsterdam, The Netherlands

† van't Hoff Laboratory, Utrecht University, Padualaan 8,
3584 CH Utrecht, The Netherlands

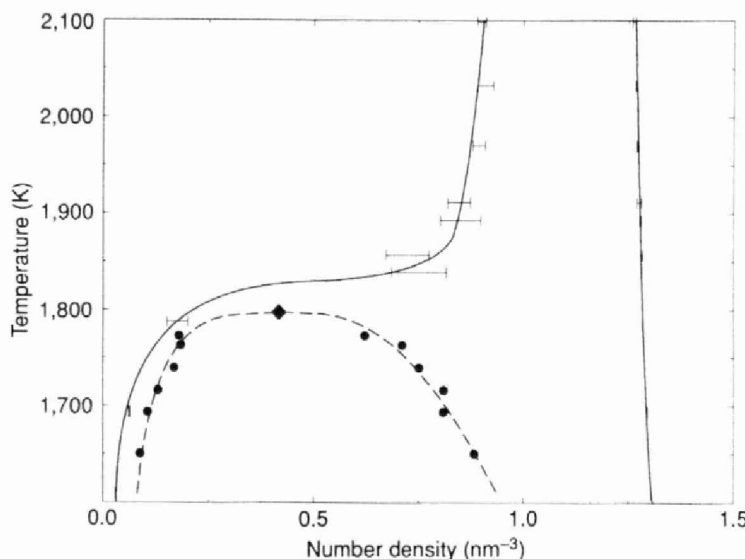


FIG. 2 Computed temperature–density phase diagram of C_{60} for temperatures in the region of 1,800 K. The solid lines are the solid–fluid coexistence lines. They were obtained by a fit to the data points (indicated by error bars) derived from free-energy calculations^{7,8} at 3,218, 1,893, 1,839, 1,788 and 1,694 K and ‘Clausius–Clapeyron’ integration⁹ between 3,218 and 1,893 K. The area between the two solid lines is a two-phase region where solid coexists with fluid. The dashed line denotes the (metastable) liquid–vapour coexistence line. It was obtained by a fit to the data points (solid circles) that were computed using the Gibbs-ensemble simulation technique of ref. 5. The solid diamond indicates the estimated location of the critical point. The fact that the critical point is located below the solid–fluid coexistence line implies that C_{60} has no liquid phase.

colloidal particles. The range of this attraction is comparable to R_g , the radius of gyration of the polymer. If R_g is larger than about one third of the radius of the colloidal particles, the phase diagram of the colloids includes a dense and a dilute disordered phase (‘liquid’ and ‘vapour’), in addition to a colloidal crystal (‘solid’). However, for shorter-ranged polymer-induced interactions, the ‘liquid’ phase disappears. In view of the short range of the pair potential shown in Fig. 1, it is natural to ask if something similar happens for C_{60} .

The phase behaviour of solid C_{60} has been studied extensively, both at low³ and high⁴ temperatures. But there are, to our knowl-

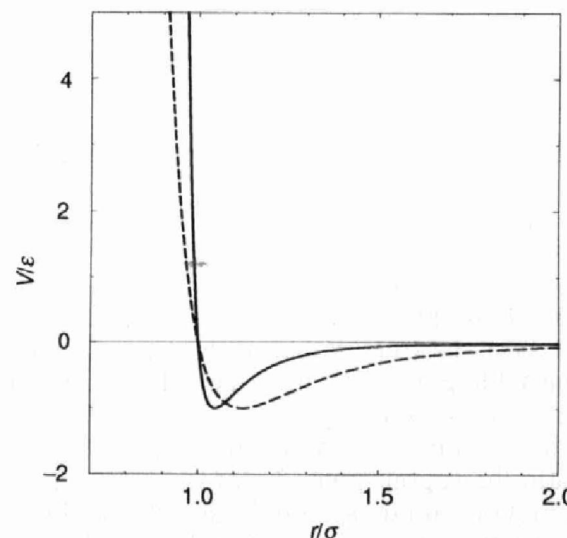


FIG. 1 A comparison of the 12–6 Lennard-Jones potential that describes the pair interaction of noble gases (dashed line), and the pair potential for C_{60} proposed in ref. 1 (solid line). The potential energy V has been expressed in units of the well depth ε . For C_{60} , $\varepsilon/k_B = 3,218$ K, where k_B is the Boltzmann constant. The intermolecular distance r is expressed in units of the effective diameter σ , defined as the distance where the pair potential crosses zero. For C_{60} , $\sigma = 0.959$ nm. In all simulations, we truncated the potential at $r = 2\sigma$ where the interaction energy is only 0.76% of the well depth.

State-of-the-art models for the phase diagram of carbon and diamond nucleation

L.M. Ghiringhelli C. Valeriani, J.H. Los, E.J. Meijer, A. Fasolino & D. Frenkel

Page 2011-2038 | Published online: 01 Dec 2010

Download citation <http://dx.doi.org/10.1080/00268970802077884>

Full Article

Figures & data

References

Citations

Metrics

Reprints & Permissions

PDF

Get access

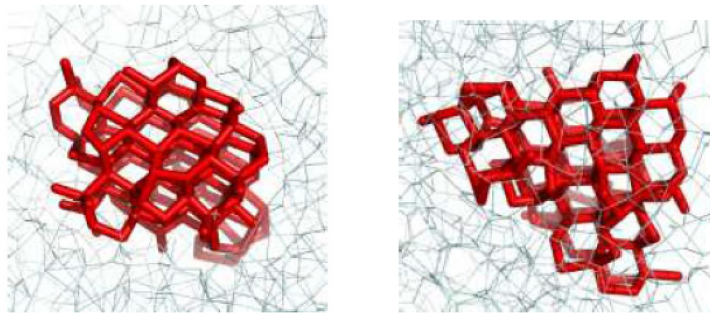


Figure 11: Two different views of the biggest cluster at state point A containing around 110 particles, surrounded by mainly 4-fold coordinated liquid particles.

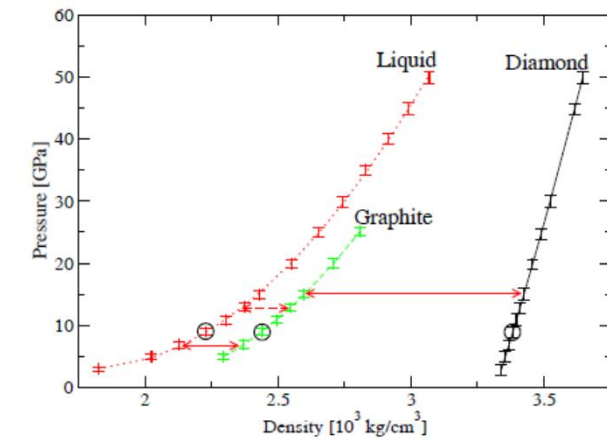
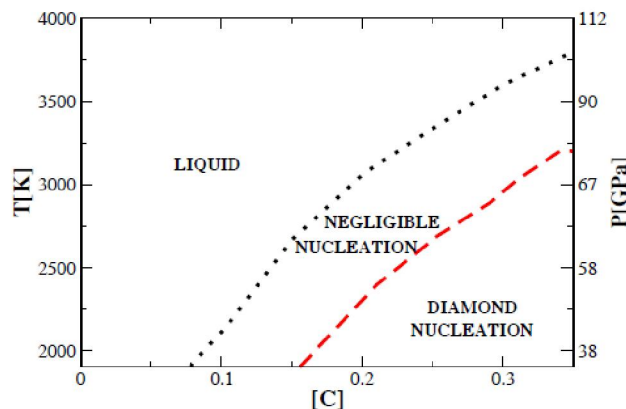


Figure 6: Equations of state at 4000K for the liquid, graphite, and diamond. The curves are quadratic polynomial fits to the data. The circles indicate the points, at 10 GPa, for which the Helmholtz free energy was determined using Eq. 6. The solid arrows connect coexisting (stable) points, i.e. liquid/graphite and graphite/diamond. The dashed arrow indicates the liquid/diamond coexisting point, with graphite metastable.

Zaključak

Molekulske simulacije u statističkoj termodinamici predstavljaju značajan doprinos razumevanu eksperimenata kao i proveri teorijskih modela

Dve najznačajnije metode su molekulska dinamika (MD) i Monte Karlo metoda (MC)

MC: Lakše ju je implementirati od MD, potrebno je manje vremena za izračunavanje, mnogo efikasnije isputuje konfiguracioni prostor nego MD jer može da "skace" kroz konfiguracioni prostor. Ne daje vremenski zavisne osobine sistema

MD: Daje vremenski zavisne osobine sistema. Troši se mnogo vremena na računanje sila, sistem može ostati zarobljen u određenom delu konfiguracionog prostora, nekada je potrebno ogromno vreme da se sistem uravnoteži tako da je MD praktično nemoguće primeniti